Microinjection Molding of Light-Guided Plates Using LIGA-Like Fabricated Stampers

Ming-Shyan Huang, Hong-Hua Ku

Department of Mechanical and Automation Engineering, National Kaohsiung First University of Science and Technology, 2 Jhuoyue Road, Nanzih, Kaohsiung City 811, Taiwan, ROC

Received 13 September 2010; accepted 26 February 2011
DOI 10.1002/app.34372
Published online 20 July 2011 in Wiley Online Library (wileyonlinelibrary.com).

ABSTRACT: This investigation explores the microinjection molding of light-guided plates (LGPs) using lithography, electroplating, and molding (LIGA)-like fabricated stampers. The 3.5-in. LGP has a thin wall (0.76 mm) and micron-sized features of truncated pyramidal prisms (70 μm wide and 38.3 μm deep, with a vertex angle of 70.5°) and v-grooves (9.8 μm deep). Stampers for LGP injection molding (IM) are fabricated precisely by combining the anisotropic wet etching of silicon-on-insulation wafers with electroforming. LGPs must have multiple quality characteristics, such as good replication effects on microfeatures and flatness of the plate. In this study, the Taguchi method and gray relational analysis are adopted to optimize the microinjection molding parameters. Various IM parameters, including mold temperature, melt temperature, holding pressure, and injection speed, are considered. Experimental results demonstrate that mold temperature and holding pressure dominate the performance. Gray relational analysis and the Taguchi method can be used to determine the optimal process parameters for LGP molding. © 2011 Wiley Periodicals, Inc. J Appl Polym Sci 122: 3446–3455, 2011

Key words: gray relational analysis; injection molding; LIGA-like; light-guided plates; microfeature; stamper

INTRODUCTION

Light-guided plate (LGP) is one of the key components of the backlight modules in liquid crystal displays. It is used to convert edge light sources, including cold cathode fluorescent lamps and light emitting diodes, into uniform planar light. The design and manufacture of the microfeatures on an LGP are the key control factors; in particular, the replication effect of the microfeatures determines their optical performance. LGPs with high illumination performance are typically manufactured using nonprinted technology. Nonprinted LGPs are generally injection-molded or hot-embossed with optical microfeatures that are integrated into the mold design. UV-LIGA, namely ultraviolet light source to expose a polymer photoresist for lithography, electroplating, and molding, is a key technology in fabricating molds. Accordingly, UV-LIGA stampers are fabricated by a process using micro-electro-mechanical systems (MEMS) that combines anisotropic wet etching of silicon-on-insulator (SOI) wafers with electroforming to yield precise two-dimensional photoresist features. Meanwhile, mask designs and high-temperature reheating are used to reform photoresist patterns into precision microfeatures. These microfeatures can be v-grooves and pyramidal structures those are designed to perform high luminance and optical quality of LGPs. However, the sharp tips of microfeatures commonly cause molding problems. For example, gas may be easily trapped within a groove area, and it may obstruct further filling of melt into the groove during injection molding (IM).[1] Venting systems are thereby necessary to place in molds to eliminate trapped air. To ease of molding, truncated pyramidal prism microfeatures of stampers that can be precisely fabricated by combining the anisotropic etching of a SOI wafer with electroforming are thus concerned for LGPs in this study.

IM, characterized with the advantages of ease of mass production and low cost, is one of the best methods for producing complex-shaped three-dimensional products and is therefore a crucially important core technology for the production of LGPs. However, IM has some inherent problems in the molding of high-quality LGPs that are associated with the replication of microfeatures and geometric precision. The main difficulty of replicating microfeatures by IM is that molten polymer in tiny cavities instantaneously freezes when it comes into

Correspondence to: M.-S. Huang (mshuang@nkfust.edu.tw).
Contract grant sponsor: The authors would like to thank the Ministry of Economics Affairs of the Republic of China, for financially supporting this research (Contract No. 98-EC-17-A-07-S1-108).

contact with the relatively cold cavity wall.[2] This phenomenon results in a massive increase in the polymer's viscosity, which can reduce its flow ability in microsized channels; thereby defeats such as short shot occur. Many researchers have investigated the importance of melt and mold temperature, injection speed, and pressure in improving microinjection molding quality. Liou and Chen[3] have studied IM of polymer microsized and submicron-sized structures with high aspect ratios and concluded that the mold temperature determines the success of the IM of microsized and submicron-sized walls. Further, the best replication results were achieved when the melt and mold temperatures exceeded their normal values.[4] In particular, the mold temperature can be sometimes close to the melt temperature or the glass transition temperature.[5–7] The injection pressure and the injection speed also affect the achievable aspect ration of the microsized and submicron-sized walls. Replication quality optimization may be generated by increasing the injection speed and holding pressure. For instance, Xu et al.[8] reported that the filling lengths in the microsized channels were affected by injection speed, mold temperature, and channel location. A high injection speed or high mold temperature resulted in a longer filling length. Also, Sha et al.[9] in their study concluded that in general high melt and mold temperatures, and high injection speed have a positive effect on the melt flow in very small cavities. However, Griffiths et al.[10] suggested that even an increase of melt temperature and injection speed improves the polymer flow due to a reduction of material viscosity and shear stress, selection an appropriate window is important in microinjection molding due to its effects on the melt flow and the possibility of preventing the occurrence of polymer degradation.

To easily find the factors which affect microinjection molding quality and to obtain processing parameters which can improve quality, the Taguchi method was utilized in this study. Taguchi method has been used widely in engineering analysis to optimize the performance characteristics within the combination of design parameters. The method introduces an integrated approach that is simple and efficient to find the best range of designs for quality, performance, and computational cost.[11] However, the Taguchi method has been developed to target a single quality by designing experiments to optimize process parameters. In the LGP microinjection molding process, finding the ideal process parameters and focusing on multiple quality characteristics is difficult but usually necessary. When various related quality characteristics are examined, experimental data may be contradictory, and data analysis may be difficult. The gray system theory proposed by Deng[12] has been proven to be useful for solving the problems of poor, insufficient, and uncertain information.[13] Gray relational analysis based on this theory can further be effectively utilized to elucidate the complex interrelationship among the designed performance characteristics. Gray relational analysis has recently become a powerful tool for analyzing processes with multiple performance characteristics. Based on this analysis, the gray relational grade is favorably defined as an index of the multiple performance characteristics.

ANALYTICAL METHOD

Signal-to-noise ratio

To analyze the effects of processing parameters on the replication of the microfeatures of an injection-molded LGP, the Taguchi method was adopted. The signal-to-noise (S/N) ratio was utilized to measure deviation in quality from the desired target. The S/N ratio, rather than averages of the experimental results, was used to optimize the parameters

$$\eta = -10\log(\mathrm{MSD}), \tag{1}$$

where *MSD* is the mean-squared deviation of output characteristic. The *S/N* ratio of characteristics can be divided into three types in the engineering analysis—nominal is best, smaller is better, and larger is better—when the quality characteristics are continuous. Since the study objectives are to identify the optimal settings that minimize replication errors in the LGP microfeatures and LGP flatness, a smaller-is-better *S/N* ratio quality characteristic is adopted. The *MSD* of a smaller-is-better quality characteristic can be expressed as

$$\mathrm{MSD} = \frac{1}{n}\sum_{i=1}^{n} \Delta Y_i^2, \tag{2}$$

where ΔY_i is the average difference between the measured value and the target value for the ith sample, and n is the total number of samples. Since $-\log$ is a monotonically decreasing function, the *S/N* value should be maximized. Hence, the *S/N* values are calculated using eqs. (1) and (2). Replication errors in LGP microfeatures and in LGP flatness as functions of the process parameters of mold temperature, melt temperature, holding pressure, and injection speed, are analyzed using the orthogonal array $L_9(3^4)$ via Taguchi method and the *S/N* ratios.

Gray relational analysis

The gray relational analysis is composed of two steps, which are (1) generation of gray relations and (2) computation of gray relational coefficient and gray

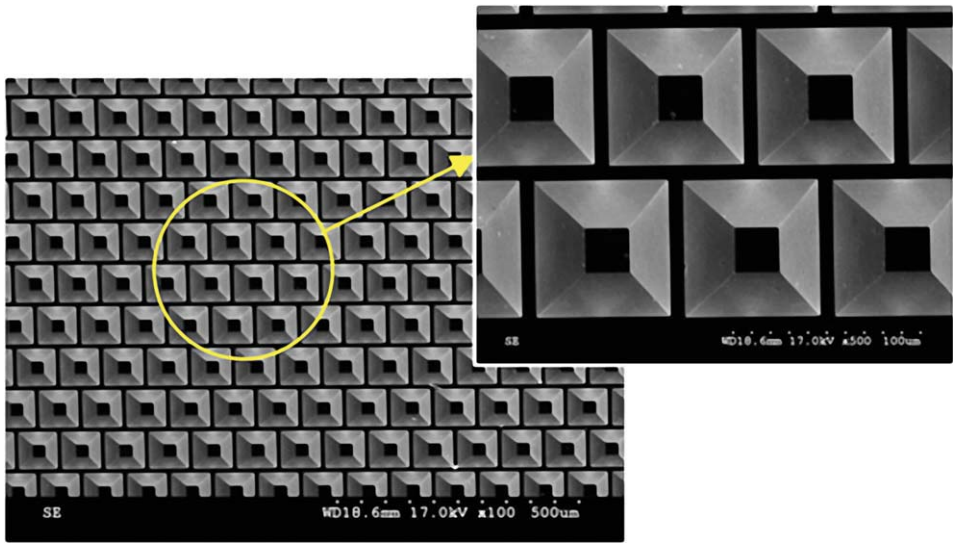

Figure 1 SEM plot of LGP stampers. [Color figure can be viewed in the online issue, which is available at wileyonlinelibrary.com.]

relational grade. In the first step, data that are related to a group of sequences must be preprocessed by gray relational generation.[12] A linear data preprocessing method for the *S/N* ratio is expressed as

$$x_i^*(k) = \frac{x_i(k) - \min\limits_{\forall k} x_i(k)}{\max\limits_{\forall k} x_i(k) - \min\limits_{\forall k} x_i(k)} \tag{3}$$

where x_i^* (k) is the sequence after data processing, x_i (k) is the original *S/N* ratio sequence, $\max\limits_{\forall k} x_i(k)$ is the largest value of x_i (k), and $\max\limits_{\forall k} x_i(k)$ is the smallest value of x_i (k).

In the second step, a gray relational coefficient can be calculated using the preprocessed sequences. The gray relational coefficient is defined as follows:

$$\gamma_{0,i}(k) = \frac{\Delta\min + \varsigma\Delta\max}{\Delta_{0,i}(k) + \varsigma\Delta\max} \tag{4}$$

where $\Delta_{0,i}$ (k) is the sequence of deviations associated with the reference sequence x_0^* (k) and the comparability x_i^* (k), where $\Delta_{0,i}(k) = \left|x_0^*(k) - x_i^*(k)\right|$ is the absolute value of the difference between x_0^* (k) and x_i^* (k),

$$\Delta\max = \max_{\forall i} \max_{\forall k} \left|\Delta_{0,i}(k)\right| \tag{5a}$$

$$\Delta\min = \min_{\forall i} \min_{\forall k} \left|\Delta_{0,i}(k)\right| \tag{5b}$$

ς is the distinguishing coefficient between 0 and 1, and is set 0.5 herein.

The coefficient ς is defined to specify the strength of the relationship between the reference sequence x_0^* (k) and the comparability sequence x_i^* (k). The gray relational grade is a weighted sum of the gray relational coefficients. It is defined as,

$$r_{0,i} = \frac{1}{n}\sum_{k=1}^{n} \gamma_{0,i}(k) \tag{6}$$

The gray relational grade $r_{0,i}$ represents the degree of the correlation between the reference sequence and the comparability sequence. If a particular comparability sequence is more important than another comparability sequence to the reference sequence, then the gray relational grade for the former comparability sequence will exceed other gray relational grades. Accordingly, gray analysis actually measures the absolute value of the difference between sequences and can be used to measure approximately the correlation between sequences.

EXPERIMENTAL METHODS

Fabrication of LGP stampers using LIGA-like process

The LGP stamper is electroformed from a master whose surface has been patterned with the truncated pyramid prisms (see Fig. 1). The original design of truncated pyramid prisms is the 70 μm for width, the 38.3 μm for height, and the 70° for vertex angle and 10 μm for pitch. The stamper is installed in a fan-gated mold base for microinjection molding. The mold has two cavities symmetrically located on the opposite sides of the sprue. Both cavities have the same pattern of microtruncated pyramid prisms. The two-plated mold used to the microinjection molding studies is shown in Figure 2. The detailed steps are described as follows.

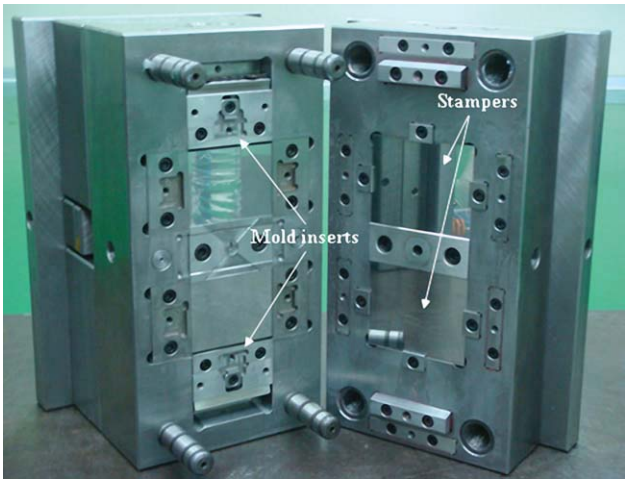

Figure 2 Injection mold. [Color figure can be viewed in the online issue, which is available at wileyonlinelibrary.com.]

Truncated square pyramidal prisms were precisely fabricated as microfeatures on a 3.5-in. stamper by wet chemical etching on a silicon wafer.[14] Figure 3 presents a schematic flowchart of stamper fabrication. Wet chemical etching using anisotropic etchants, including aqueous potassium hydroxide (KOH) and tetramethylammonium hydroxide (TMAH), are applied to fabricate three-dimensional microfeatures on silicon wafers. The feature geometry after etching is bounded by (111) crystalline planes. The etching depth of the feature geometry is controlled by setting the layer thickness of the (100) SOI wafer to fabricate truncated pyramidal prisms precisely with a vertex angle of 70.5°. A thin layer of silicon dioxide (SiO_2) is grown on the SOI by thermal oxidation. On etched wafers are then deposited thin layers of titanium (Ti) and silver (Ag) using E-beam evaporation as a seed layer for electroforming. Nickel-based electroforming is performed to transcribe the silicon features onto a metal plate. It is followed by backside grinding to the desired thickness and flatness. The stamper is finally released by KOH wet etching.

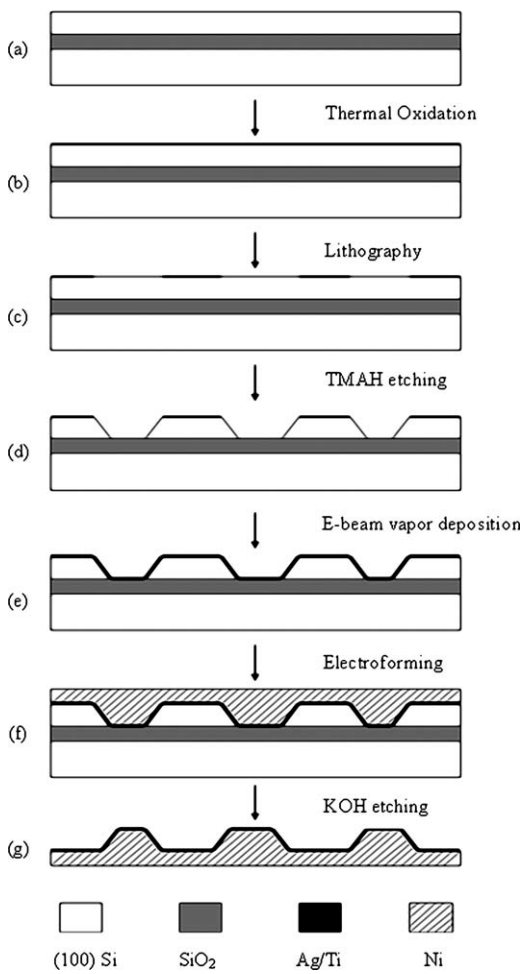

Figure 3 Flowchart of stamper fabrication.[14]

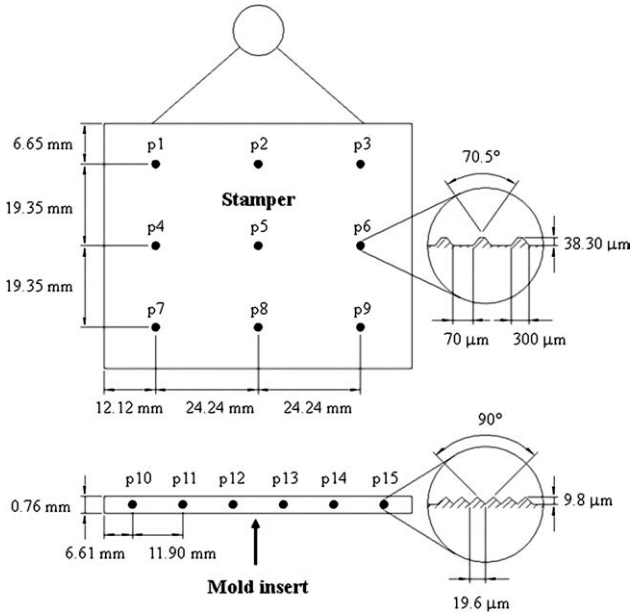

Figure 4 Microfeatures and their measured locations on a 3.5-in. LGP stamper and mold insert.

Material, geometry of molded parts, mold design, molding machine, and measurement of quality

The plastic that was used in this experiment was poly(methyl methacrylate) (PMMA; Kuraray GH-1000S) with a glass transition temperature of 104°C.

TABLE I
Specifications of Taylor Hobson Surface Profiler

Specification	Taylor Hobson
Model	Taylsurf Laser 635
Scanning distance	0.5 mm
Scanning speed	0.1 mm/s
Probe radius	2.1 μm
Probe angle	40.2°

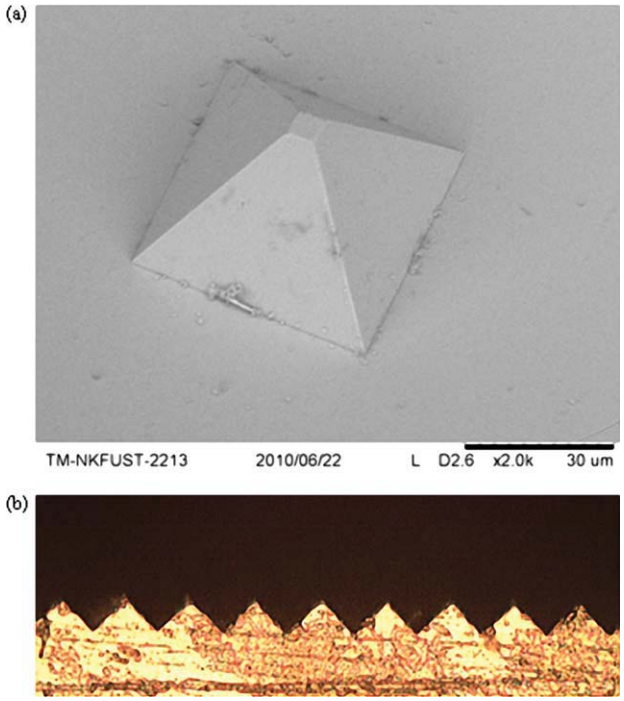

Figure 5 Microfeatures on stamper: (a) SEM micrographs of truncated pyramidal prisms (width = 70 μm; height = 38.3 μm; vertex angle = 70.5°) and (b) optical microscopic image of v-grooves (pitch = 19.6 μm; height = 9.80 μm; angle = 90°). [Color figure can be viewed in the online issue, which is available at wileyonlinelibrary.com.]

The molded part is a flat LGP that is 73 mm long, 58 mm wide, and 0.76 mm thick. This two-cavity mold is designed with a fan-shaped gate that is 40 mm wide and 0.4 mm thick. Figure 2 presents the structure of the mold base that is used in IM, whereas the mold insert with v-grooves are put adjacent to the edge of the stamper with truncated pyramidal prisms. The microfeatures are v-grooves that are 9.8 μm deep and have a pitch of 19.6 μm (Fig. 4). Under each molding condition, two LGPs are sampled. After the samples had been cooled for 24 h after molding the samples were stored for 24 h at room temperature, the microfeatures of the LGP are measured using a probe-touching surface profiler (Taylor Hobson Surface profiler). Table I lists the specifications of the employed measurement device. The device is the commonly used to measure

TABLE II
Microstructure of LGP Stamper

Position	Truncated pyramidal prisms (μm)	v-Grooves (μm)
p1	38.21	
p2	37.83	
p3	37.93	
p4	38.55	
p5	38.85	
p6	38.49	
p7	38.21	
p8	38.45	
p9	37.19	
p10		9.8
p11		9.8
p12		9.8
p13		9.8
p14		9.8
p15		9.7
Average	38.30	9.8
Std	0.32	0.04

TABLE III
Control Factors and Levels Used in Taguchi Experiments

	Level		
Control factor	1	2	3
A. Mold temperature (°C)	70	85	100
B. Melt temperature (°C)	250	260	270
C. Holding pressure (MPa)	40	50	60
D. Injection speed (mm/s)	300	450	600

TABLE IV
The L_9 Orthogonal Array and Experimental Results

	Replication error								
	Truncated pyramid prisms (μm)			v-Grooves (μm)			Flatness (mm)		
No.	S1	S2	S3	S1	S2	S3	S1	S2	S3
1	0.30	0.32	0.30	4.2	4.3	4.3	0.057	0.053	0.056
2	0.13	0.14	0.14	3.8	3.6	3.7	0.082	0.078	0.079
3	0.09	0.09	0.13	3.1	3.2	3.2	0.159	0.156	0.157
4	0.08	0.09	0.10	2.6	2.6	2.8	0.155	0.152	0.153
5	0.09	0.10	0.10	2.7	2.9	2.7	0.244	0.246	0.249
6	0.09	0.09	0.08	2.5	2.4	2.5	0.053	0.051	0.056
7	0.08	0.08	0.08	2.3	2.6	2.3	0.165	0.178	0.173
8	0.11	0.11	0.10	2.2	1.9	2.1	0.067	0.063	0.061
9	0.08	0.08	0.09	2.6	2.5	2.5	0.276	0.268	0.271

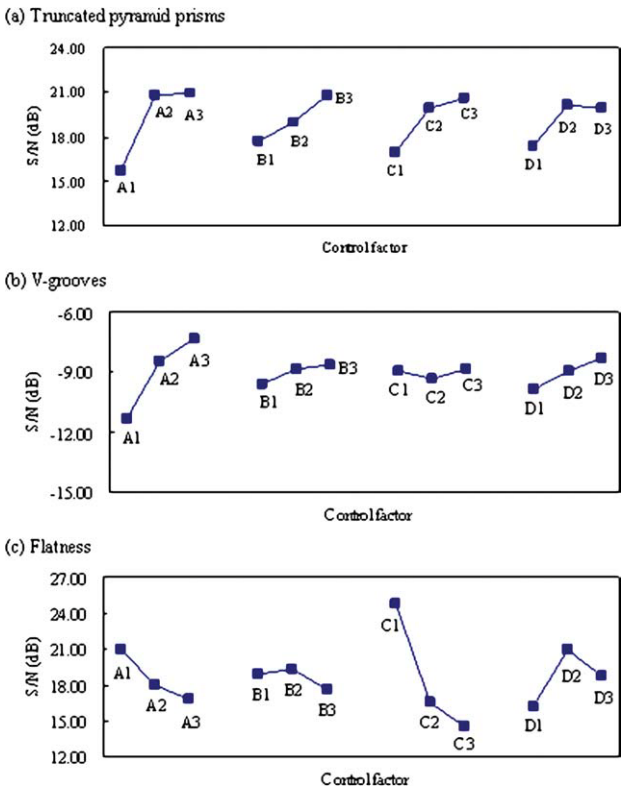

Figure 6 S/N response diagram.

microscaled structures and operates efficiently. However, the accuracy of measurements is limited by the radius of the probe and the geometry of the microstructures. The accurate measurement of microstructures requires a strategy for compensating measurement errors.[15]

Figure 4 presents the positions on the stamper and mold insert where the truncated pyramidal prisms and v-grooves were measured, respectively. Figure 5(a) shows the SEM micrographs of LIGA-like fabricated truncated pyramidal prisms on stampers (width = 70 μm; height = 38.30 μm; vertex angle = 70.5°). Figure 5(b) displays an optical microscope graph of micromachined v-grooves on the side of the LGPs (pitch = 19.6 μm; height = 9.8 μm; vertex angle = 90°). Table II presents the measurements of these two microfeatures.

Molding was performed using a high-speed closed-loop hybrid IM machine (FCS AF-100). The machine provided a clamping force of up to 100 tons. The screw diameter was 28 mm, and the maximum injection volume was 92 cm^3. Under each set of processing conditions, 10 shots were made to ensure that IM process was stable before the samples were collected. If no significant variation of molding conditions was observed in these first 10 runs, then the molded parts following the next three runs were collected as samples to characterize products.

Taguchi parameters design

Experiments are executed according to an L_9 orthogonal array for IM. Table III shows the control factors and their levels set in the Taguchi experiments. According to the short-shot experiment, the specification limits of the employed machine and polymer materials processing range provided by vendors, the following ranges of control factors were set: mold temperature (A, 70–100°C); melt temperature (B, 250–270°C); holding pressure (C, 40–60 MPa);

TABLE V
Sequences of *S/N* Ratios

No.	Truncated pyramid prisms	v-Grooves	Flatness
1	10.26	−12.60	25.14
2	17.28	−11.37	21.97
3	19.57	−10.01	16.06
4	20.88	−8.52	16.29
5	20.28	−8.84	12.17
6	21.23	−7.84	25.45
7	21.94	−7.62	15.29
8	19.43	−6.32	23.92
9	21.57	−8.08	11.32

TABLE VI
Sequences After Preprocessing of Data

No.	Truncated pyramid prisms	v-Grooves	Flatness
Reference sequence	1.000	1.000	1.000
Comparability sequence			
1	0.000	0.000	0.978
2	0.601	0.197	0.754
3	0.797	0.412	0.336
4	0.909	0.649	0.351
5	0.858	0.598	0.060
6	0.939	0.758	1.000
7	1.000	0.793	0.281
8	0.785	1.000	0.891
9	0.968	0.721	0.000

TABLE VII
Deviation Sequences

Deviation sequences	$\Delta_{o,i}(1)$	$\Delta_{o,i}(2)$	$\Delta_{o,i}(3)$
No. 1, $i = 1$	1.000	1.000	0.022
No. 2, $i = 2$	0.399	0.803	0.246
No. 3, $i = 3$	0.203	0.588	0.664
No. 4, $i = 4$	0.091	0.351	0.649
No. 5, $i = 5$	0.142	0.402	0.940
No. 6, $i = 6$	0.061	0.242	0.000
No. 7, $i = 7$	0.000	0.207	0.719
No. 8, $i = 8$	0.215	0.000	0.109
No. 9, $i = 9$	0.032	0.279	1.000

TABLE VIII
Calculated Gray Relational Coefficients and Gray Relational Grades for Nine Comparability Sequences

No. (comparability sequence)	Gray relational coefficient			Gray relational grade
	Truncated pyramid prisms	v-Grooves	Flatness	
1	0.333	0.333	0.957	0.541
2	0.556	0.384	0.670	0.537
3	0.712	0.460	0.429	0.534
4	0.846	0.588	0.435	0.623
5	0.779	0.555	0.347	0.560
6	0.892	0.673	1.000	0.855
7	1.000	0.708	0.410	0.706
8	0.700	1.000	0.821	0.840
9	0.941	0.642	0.333	0.639

injection speed (D, 300–600 mm/s). Table IV presents the results of nine experimental runs based on an orthogonal array, L_9, of four experimental factors, each with three levels.

ANALYSIS AND DISCUSSION

The algorithm associated with gray relational analysis that was used in this study to determine the optimal combinations of the IM parameters for LGP has six steps—convert experimental data into *S/N* values; normalize the *S/N* ratio; calculate the corresponding gray relational coefficients and the gray relational grade; perform a statistical analysis of variance (ANOVA); select the optimal levels of the cutting parameters; conduct confirmatory experiments.

Effects of molding factors on replication accuracy

Table IV presents the L_9 experimental results of the IM the LGPs. Columns 2–4 and 5–7 list errors in replicating the depth of truncated pyramidal prisms and v-grooves, respectively. Also, columns 8–10 present LGP flatness. Among the nine possible combinations in Taguchi's orthogonal array, the best combination for the truncated pyramidal prisms was that in Exp. No. 7; that for the v-grooves was that in Exp. No. 8, and that for flatness was in Exp. No. 1. Moreover, the *S/N* response diagrams (Fig. 6) show that mold temperature (A) was the most influential factor for the replication quality of truncated pyramidal prisms, followed by holding pressure (C), melt temperature (B), and injection speed (D). The optimal process parameters were $A_3B_3C_3D_2$ for minimum replication errors on truncated-pyramid-prism heights from the IM process. Mold temperature (A), injection speed (D), and holding pressure (C) affect the replication quality of v-grooves, and the optimal process parameters were $A_3B_3C_3D_3$. As to the flatness, the most significant control factors were holding pressure (C), injection speed (D), and mold temperature (A) in sequence, and the optimal process parameters were $A_1B_2C_1D_2$. The optimal process parameters for the replication qualities of truncated pyramidal prisms and v-grooves are the same except injection speed. It is due to the fact that the v-groove microfeatures are located far from the gate and requires fast injection speed to assure high replication quality especially for thin-walled molding. As to the quality of flatness, holding pressure is most significant that determines the geometry quality of injection-molded parts. In such a case, to seek the ideal process parameters for these multi-quality characteristics is generally required but difficult due to experimental data that may be contradictory. To resolve this problem, the gray relational analysis that can elucidate the complex interrelationship among the designed performance characteristics is then introduced in this study.

TABLE IX
Response Table for Gray Relational Grades

Control factor	Level 1	Level 2	Level 3	Max-Min
A	0.537	0.680	**0.728**	0.191
B	0.623	0.646	**0.676**	0.052
C	**0.746**	0.599	0.600	0.146
D	0.580	**0.699**	0.666	0.119

Average gray relational grade = 0.518. Bold means the maximal value in the column.

TABLE X
Results of Analysis of Variance

Symbol of variation	Sum of square	Degree of freedom	Mean square	Pure of sum squares	Contribution percentage (%)
A	0.059	2	0.030	0.059	46.04
B	0.004	2	0.002	0.004	3.22
C	0.043	2	0.021	0.043	33.10
D	0.023	2	0.011	0.023	17.64
Pooled error		0			
Total	0.128	8			100.00

TABLE XI
Optimal Combination

	Best combination	Truncated pyramid prisms (μm)	v-Grooves (μm)	Flatness (mm)
Optimal design 1	$A_3B_3C_3D_2$	38.21	7.4	0.172
Optimal design 2	$A_3B_3C_3D_3$	38.19	7.3	0.064
Optimal design 3	$A_1B_2C_1D_2$	37.99	5.5	0.055
GRA optimal design	$A_3B_3C_1D_2$	38.22	8.6	0.065

Gray relational analysis

The performance characteristics obtained from the experimental results are initially converted into an *S/N* ratio to find the results associated with the best performance and the lowest variance. For LGP microinjection molding, the replication error of microfeatures and the warpage must be minimized. Thus, the replication error of the microfeatures and flatness are of smaller-the-better type. The experimental results in Table IV are substituted into eqs. (1) and (2) to calculate the *S/N* ratios of the truncated pyramidal prisms and v-grooves, and the plate flatness, which are presented in Table V. A larger *S/N* ratio generally corresponds to better performance.

All of the original sequences of *S/N* ratios in Table V are then substituted into eq. (3) to be normalized. Table VI presents the results. $x_0^*(k)$ and $x_i^*(k)$ denote the reference sequence and comparability sequences, respectively. According to Deng (1982), larger normalized results correspond to better performance, and the maximum normalized result, one indicates the best performance.

According to Table VI, the deviation sequences are $\Delta_{0,1}(k) = \left|x_0^*(k) - x_1^*(k)\right|$, therefore $\Delta_{0,1} = (1.0000, 1.0000, 0.0225)$. The same method of calculation was

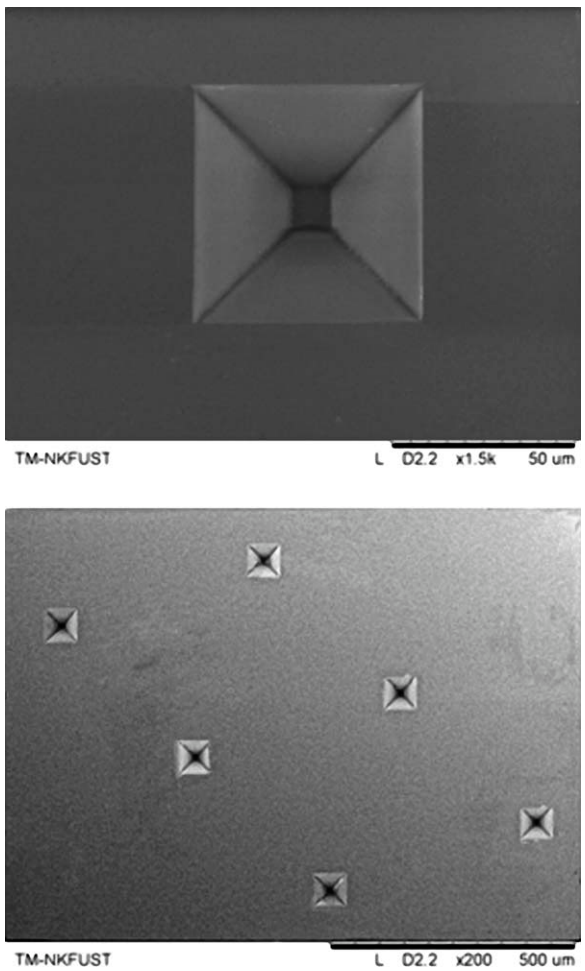

Figure 7 SEM micrographs of injection-molded truncated pyramid prisms (38.22 μm in depth; replication rate = 99.8%).

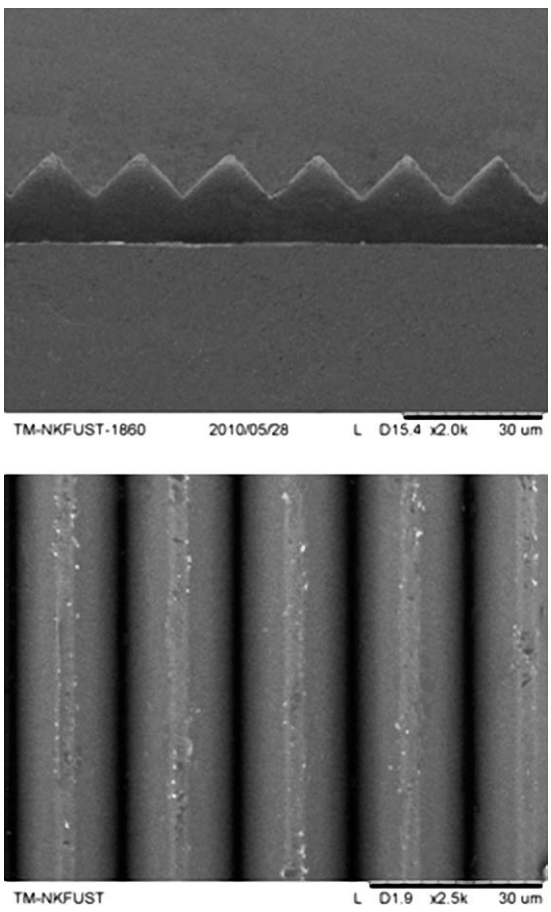

Figure 8 SEM micrographs of injection-molded v-grooves (pitch = 19.4 μm; height = 8.6 μm; replication rate = 87.8%).

applied for $i = 1$–9, and all $\Delta_{0,i}$ for $i = 1$–9 are presented in Table VII.

The data in Table VII reveal that $\Delta\max = 1.0000$, and $\Delta\min = 0.0000$. From Table VI and eq. (4), the gray relational coefficient $\gamma_{0,1}(k)$, $k = 1$–3, is calculated as (0.3333, 0.3333, 0.9570). A similar procedure is applied for $i = 1$–9. Table VIII presents the gray relational coefficients for all nine comparability sequences.

According to eq. (6), the gray relational grade $r_{0,i}$ is $(0.3333 + 0.3333 + 0.9570)/3 = 0.5412$. The gray relational grade of the comparability sequence for $i = 1$–9 can be obtained similarly and is presented in Table VIII. Accordingly, the design can be optimized with respect to a single gray relational grade rather than complex performance characteristics.

The response table of the Taguchi method is applied here to calculate the average gray relational grade for each control factor level. The calculation is performed by sorting the gray relational grades by the level of the control factor in each column of the orthogonal array and taking an average over those with the same level. Table IX is the response table. A larger gray relational grade corresponds to a better multiple performance characteristic. Hence, the level that maximized the average response is selected. From the response table of the gray relational grades (Table IX), the best combination of the control factors is A_3 (mold temperature of 100°C), B_3 (melt temperature of 270°C), C_1 (holding pressure of 40 MPa), and D_2 (injection speed of 450 mm/s).

Analysis of variance

Table X presents the ANOVA results that reveal the significance of the effect of the process parameters on the performance characteristics. The analysis of percentage contributions to the variance indicates that the control factor "*A*" (mold temperature) was the most influential factor with a contribution of 46.04%; the second most significant control factor was "*C*" (holding pressure), which was responsible for 33.10% of the variance.

Confirmatory tests

Once the optimal level of the control factors has been identified, the following step is implemented to confirm the improvement in the performance characteristics offered by this optimal combination. Table XI compares the results of the confirmation experiments obtained using the optimal IM parameters $A_3B_3C_1D_2$, as determined by the proposed method with those optimal process parameters obtained using the Taguchi method, i.e., $A_3B_3C_3D_2$, $A_3B_3C_3D_3$, and $A_1B_2C_1D_2$.

From the measurements of three injection-molded samples that were produced with optimal parameter settings, the replication of the depth of the v-grooved microfeatures is effective, with an 87.8% replication rate (against a best original value of 75.5%). Furthermore, the replication rate of the depth of the truncated pyramidal prisms is improved to 99.8%. Meanwhile, the flatness is maintained within the specified limits. Figures 7 and 8 display SEM micrographs of the injection-molded parts.

CONCLUSIONS

This study presents an effective approach for optimizing the parameters of microinjection IM 3.5-in. LGPs that are characterized by thin walls (0.76 mm) and micron-sized features of truncated pyramidal prisms (70 μm wide and 38.3 μm deep, with a vertex angle of 70.5°). Stampers for LGP IM are precisely fabricated using by UV-like technology. LGP molding depends on the successful replication of microfeatures and flatness of the plate. This investigation applies gray relational analysis for parameter optimization. The results are summarized as follows:

(1) Gray relational analysis can objectively determine the effects of the multiple performance characteristics.
(2) Based on ANOVA, the factors that mostly affect the multiple performance characteristics are mold temperature and holding pressure, which together explain 79% of performance variation.
(3) The optimal combination of the LGP IM parameters determined using the proposed method is A_3 (mold temperature of 100°C), B_3 (melt temperature of 270°C), C_1 (holding pressure of 40 MPa), and D_2 (injection speed of 450 mm/s). The corresponding confirmation test demonstrates that replication rate of v-grooved microfeatures is significantly increased by 12.3% compared with the optimal setting obtained using Taguchi method.

The authors would like to thank Dr. J. -C. Yu, our project team member, in preparing stampers for LGP injection molding. Ted Knoy is also appreciated for his editorial assistance.

References

1. Yokoi, H.; Han, X.; Takahashi, T.; Kim, W. Polym Eng Sci 2006, 46, 1140.
2. Yoshii, M.; Kuramoto, H.; Ochiai, Y. Polym Eng Sci 1998, 38, 1587.

3. Liou, A.; Chen, R. Int J Adv Manuf Tech 2006, 28, 1097.
4. Mönkkönen, K.; Hietala, J.; Paakkonen, P.; Paakkonen, E.; Kaikuranta, T.; Pakkanen, T.; Jaaskelainen, T. Polym Eng Sci 2002, 42, 1600.
5. Huang, M. -S.; Tai, N. –S. J Appl Polym Sci 2009, 113, 1345.
6. Huang, M. -S.; Yu, J. -C.; Lin, Y. –Z. J Appl Polym Sci 2010, 118, 3058.
7. Yu, M.; Young, W.; Hsu, P. Mater Sci Eng 2007, 460, 288.
8. Xu, G.; Yu, L.; Lee, J.; Koelling K. Polym Eng Sci 2005, 45, 866.
9. Sha, B.; Dimov, S.; Griffiths, C.; Packianather, M. J Mater Process Technol 2007, 183, 284.
10. Griffiths, C.; Dimov, S.; Brousseau, E.; Hoyle, R. J. Mater Process Technol 2007, 189, 418.
11. Taguchi, G. Introduction to Quality Engineering; New York: McGraw-Hill, 1990.
12. Deng, J. J Grey Syst 1989, 1, 1.
13. Chen, M.; Syu, M. Int J Adv Manuf Tech 2003, 26, 83.
14. Yu, J. -C.; Hsu, P. –K. Microsyst Technol 2009, 16, 1193.
15. Yu, J. -C.; Huang, M. -S.; Chen, C. -N. Conference of Modern Accuracy Theory and Applications 2009, Taoyuan, Taiwan.